Supplementary Information (SI) for Dalton Transactions.


# Supplementary Information

## Structure and Luminescent Properties of Acetamidinium and Imidazolium-Based Copper Halides

Andrey A. Petrov[1,2], Luyi Chen[1], Mingming Li[1*], Sergey A. Fateev[1*]

[1] Faculty of Materials Science, Shenzhen MSU-BIT University, 518172 Shenzhen, China

[2] Laboratory of New Materials for Solar Energetics, Department of Materials Science, Lomonosov Moscow State University, 119991 Moscow, Russia

[*]Corresponding authors: Sergey A. Fateev (saf1al@yandex.ru), Mingming Li (lmmhfut@163.com)

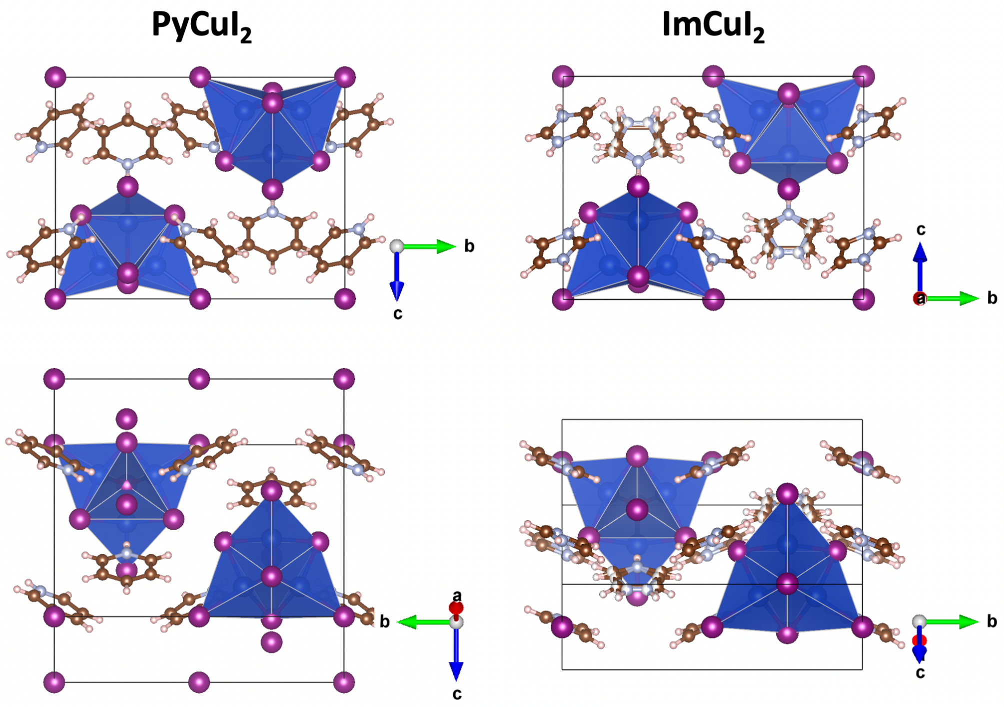


Figure S1. Crystal structures of $(HPy)_3[Cu_3I_6]$ (left) and $ImCuI_2$ (right) in different projections.

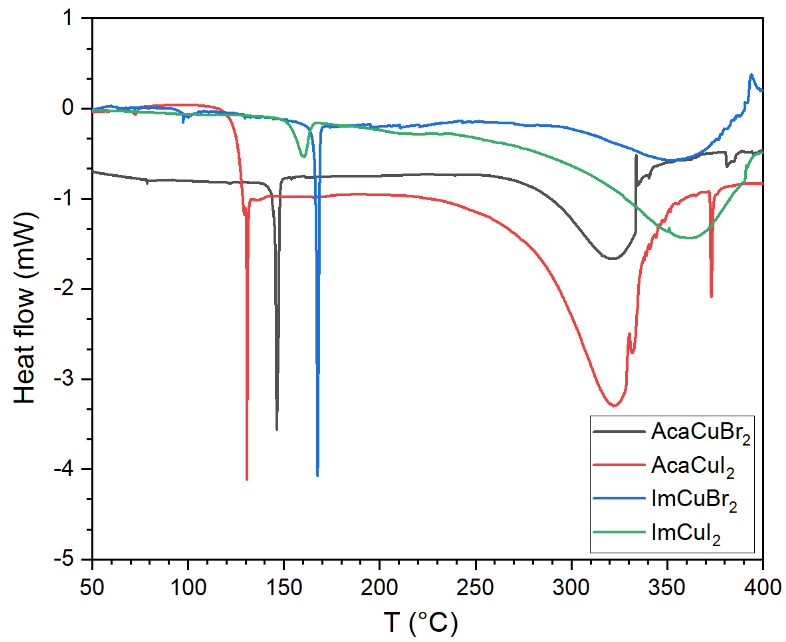


Figure S2. DSC for $AcaCuBr_2$, $AcaCuI_2$, $ImCuBr_2$ and $ImCuI_2$

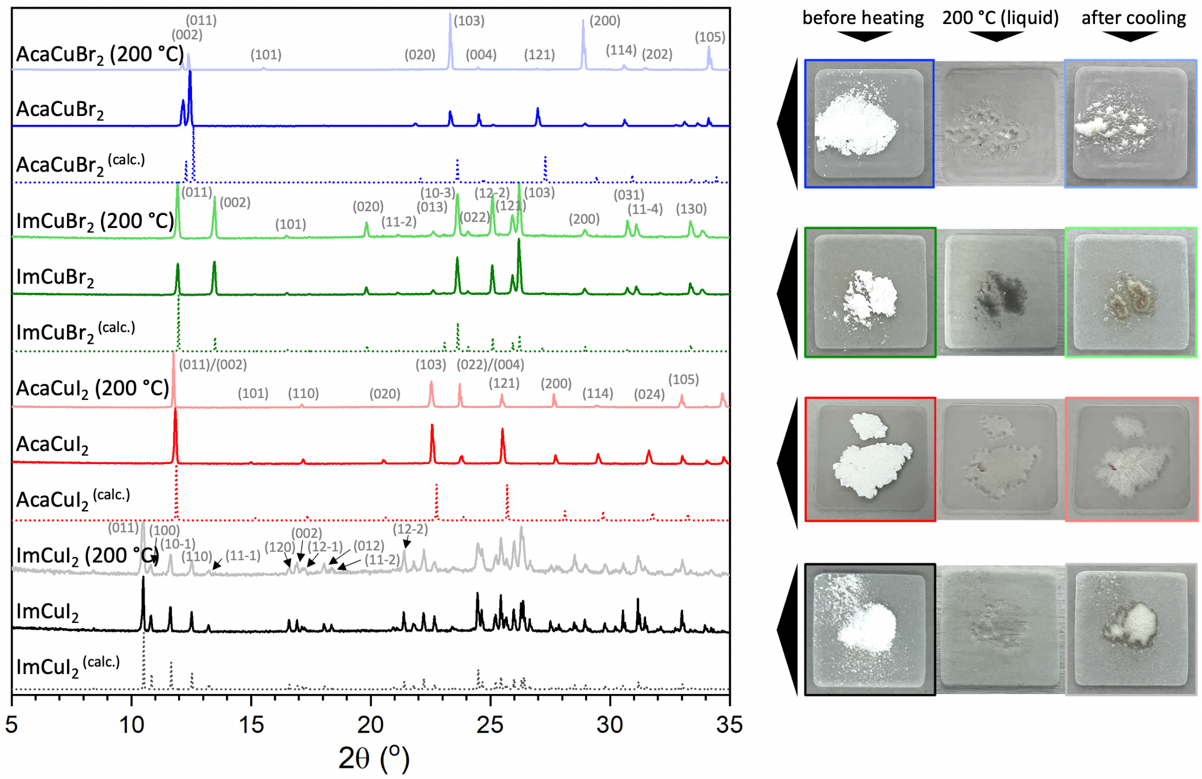


Figure S3. Experimental powder X-ray diffraction patterns of $AcaCuI_2$, $ImCuI_2$, $AcaCuBr_2$, and $ImCuBr_2$ before and after heating at 200 °C for 3 min, together with calculated patterns (dotted) and corresponding photographs of the samples in XRD cuvettes. The slight discrepancy observed between the simulated and experimental patterns for $ImCuBr_2$ (T = 100 K) arises from a phase transition near -17 °C, as confirmed by DSC measurements (Fig. S12) and by profile analysis of the PXRD pattern (Fig. S13) collected at room temperature.

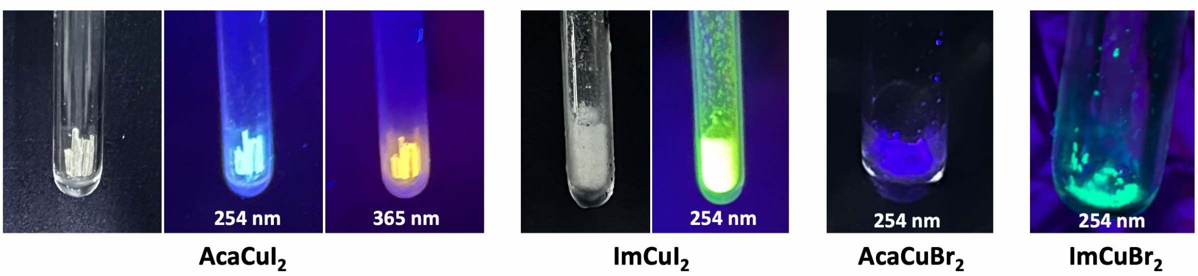


Figure S4. Photoluminescence of $AcaCuI_2$, $ImCuI_2$, $AcaCuBr_2$, and $ImCuBr_2$ halocuprates at 77K.

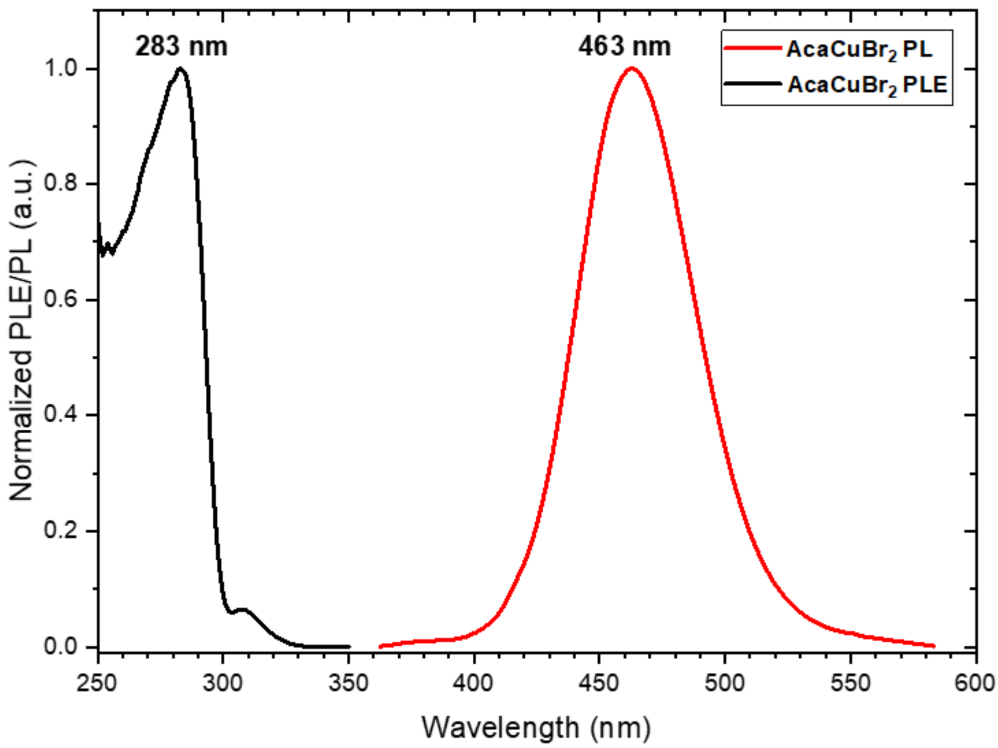


Figure S5. PLE & PL spectra of (Aca)$CuBr_2$ at 77K.

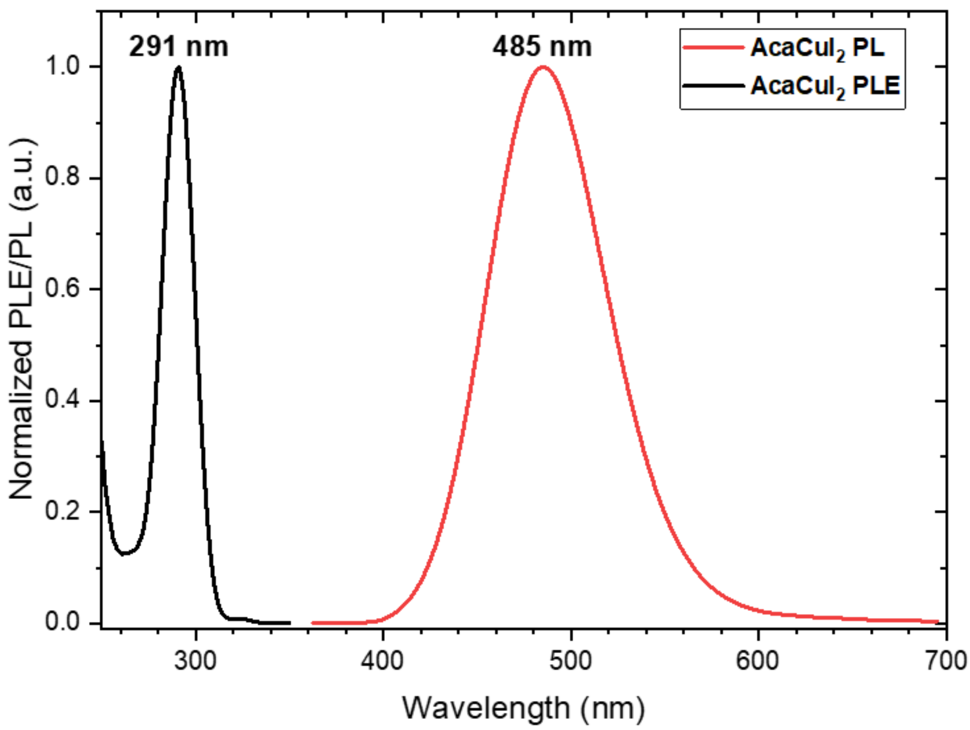


Figure S6. PLE & PL spectra of Aca$CuI_2$ at 77K.

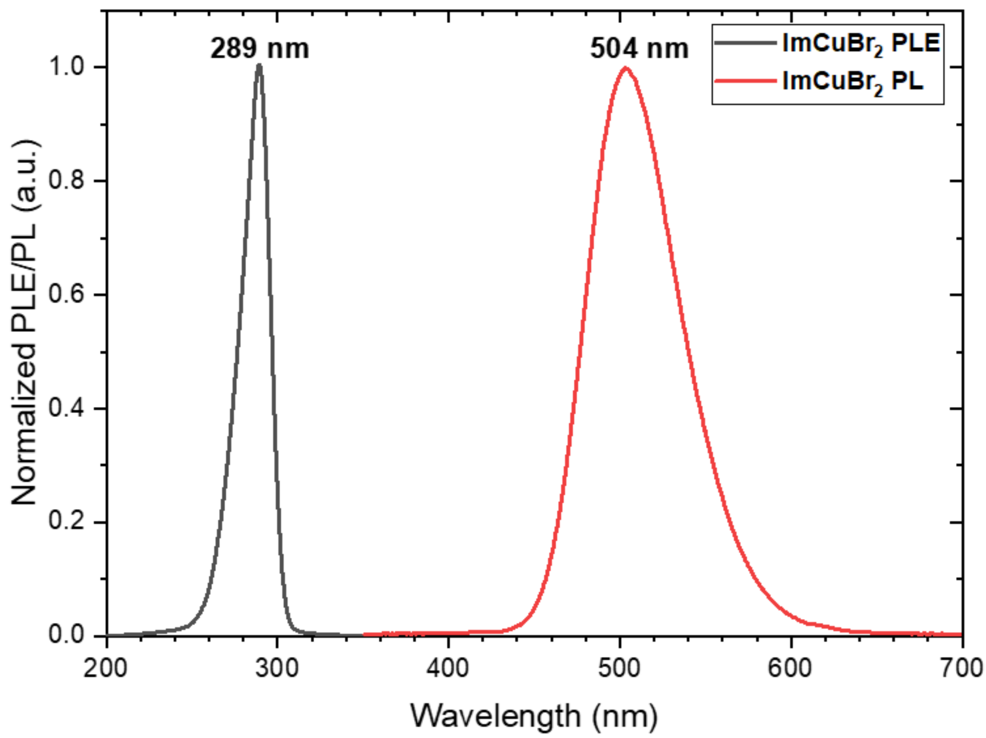


Figure S7. PLE & PL spectra of $ImCuBr_2$ at 77K.

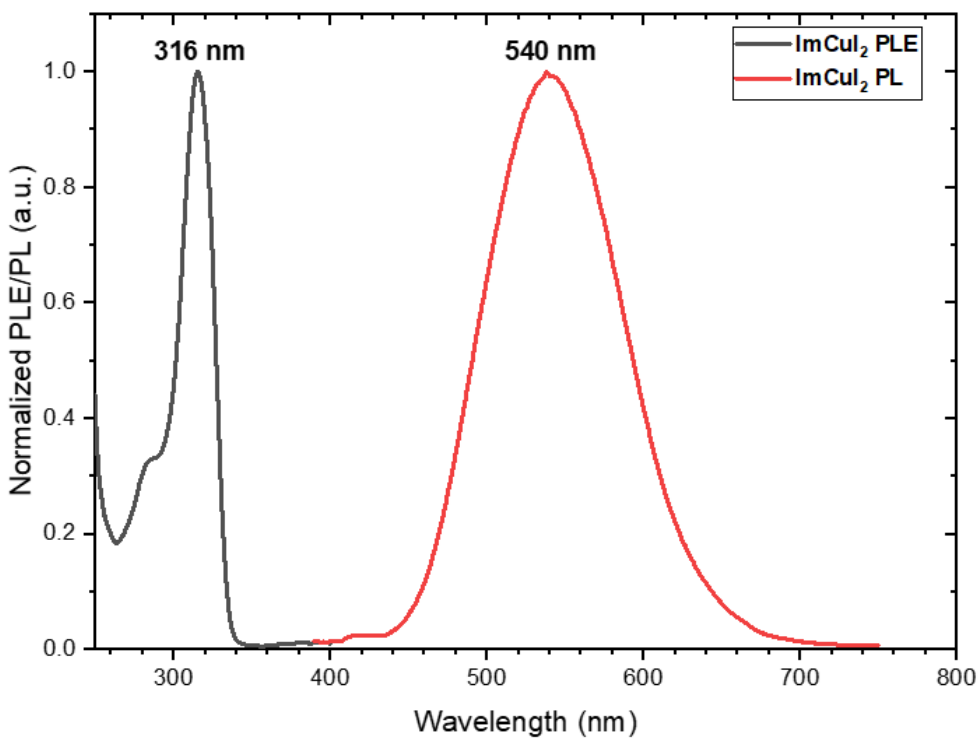


Figure S8. PLE & PL spectra of $ImCuI_2$ at 77K.

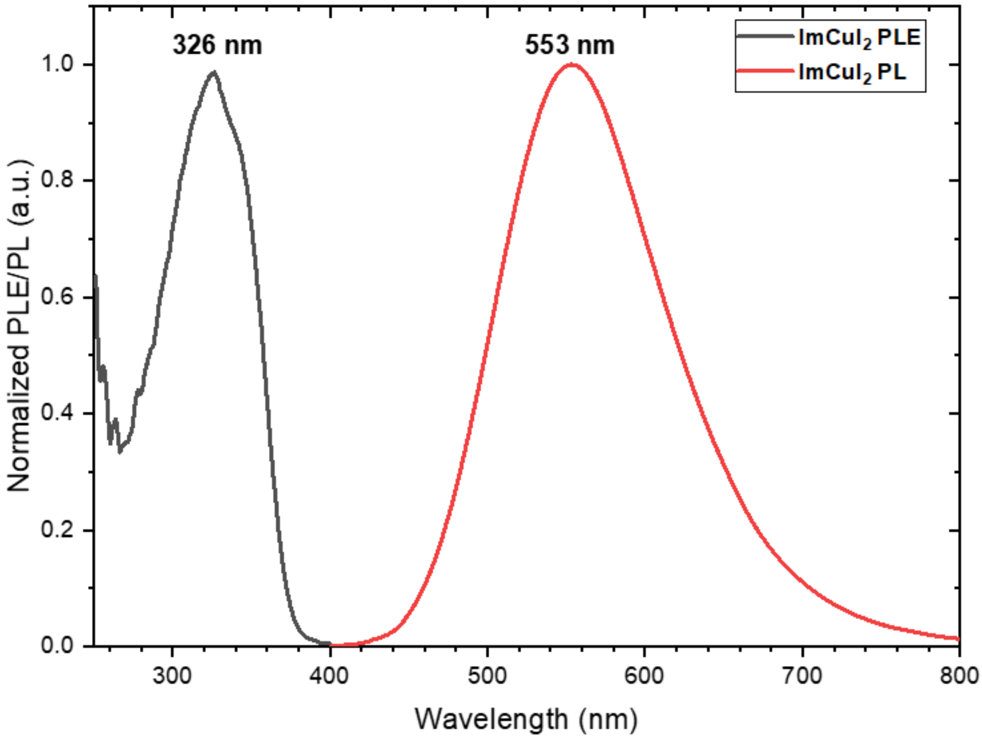


Figure S9. PLE & PL spectra of $ImCuI_2$ at RT.

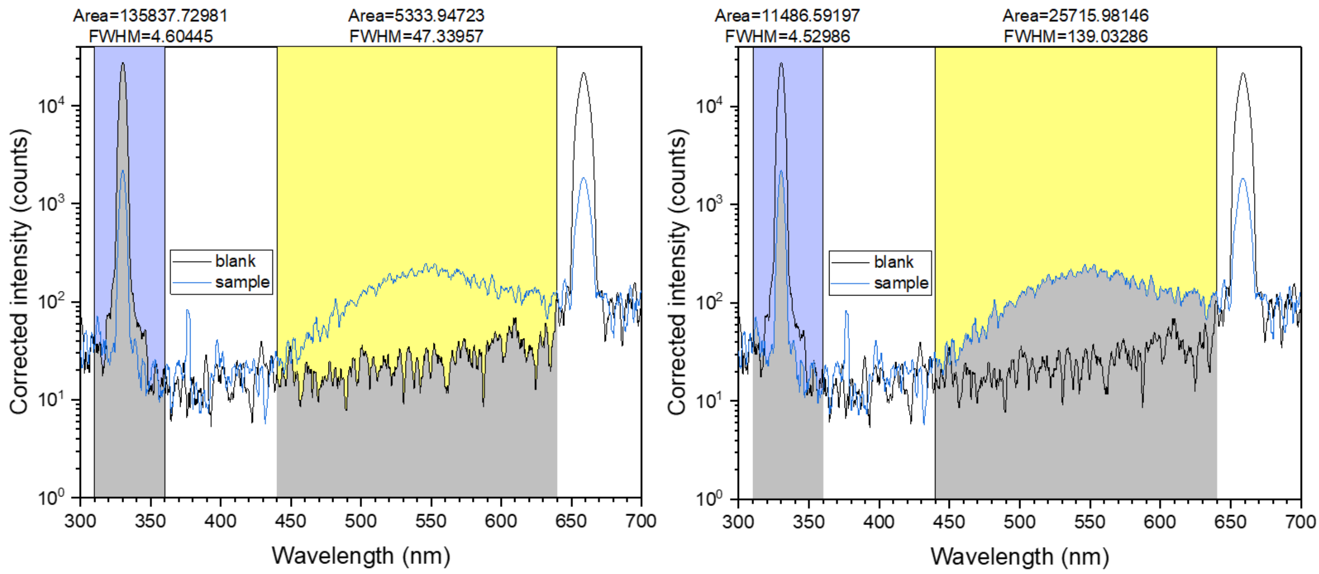


Figure S10. The illustration of photoluminescence quantum yield (PLQY) calculation. The left panel shows the integrals of excitation ($L_a$) and emission ($E_a$) for the blank (an empty integrating sphere with the sample holder and quartz cover). The right panel shows the corresponding integrals ($L_c$ and $E_c$) for the sample (integrating sphere with $ImCuI_2$ powder in the sample holder covered by quartz). The calculated PLQY is about 16.4%.

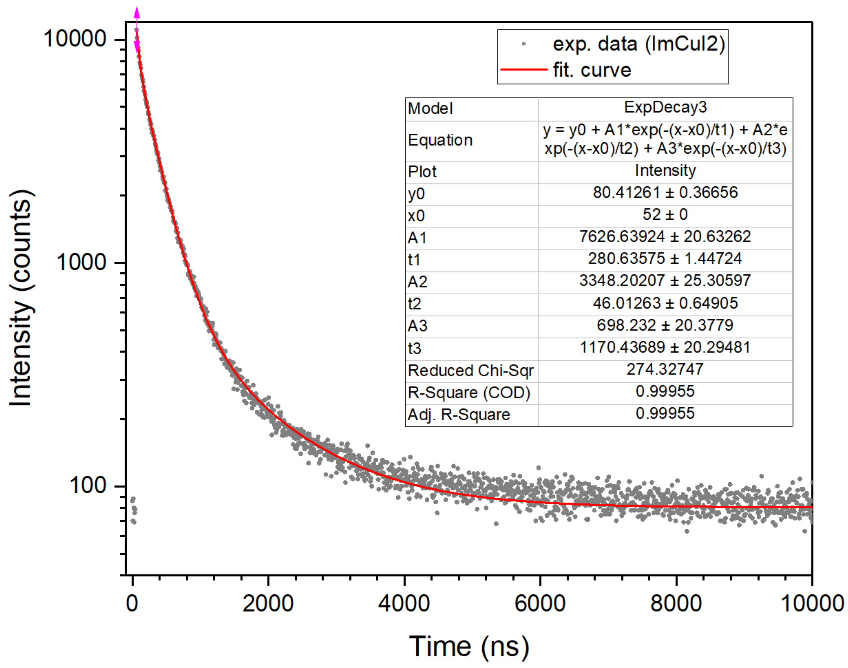


Figure S11. Time-resolved photoluminescence decay of $ImCuI_2$ at room temperature together with the triple-exponential fit, yielding lifetimes $\tau_1$ = 280.6 ns (65.3%), $\tau_2$ = 46 ns (28.7%), and $\tau_3$ = 1170 ns (6%).

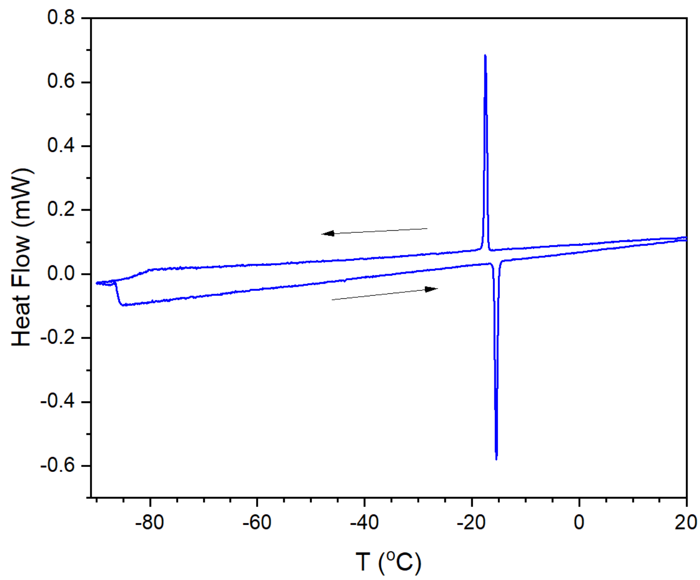


Figure S12. DSC curve for $ImCuI_2$ crystals indicating phase transition.

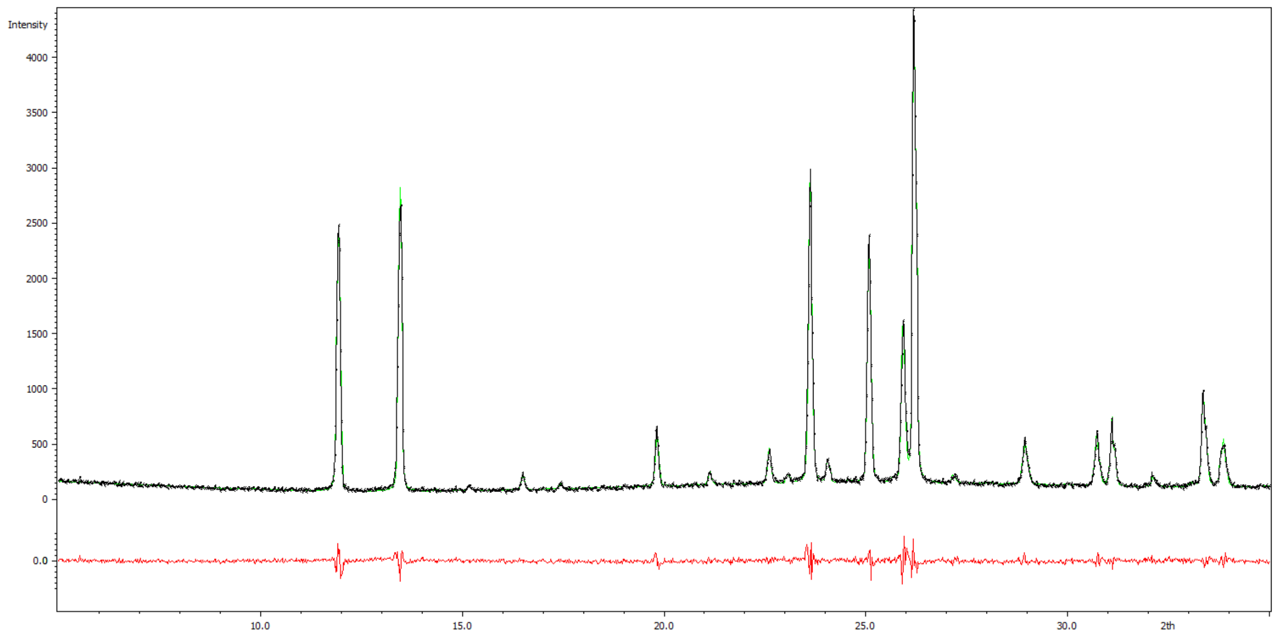

Figure S13. Profile analysis of PXRD pattern of $ImCuBr_2$ measured at room temperature (the experimental curve plotted in black, the calculated curve in green, and the difference curve in red).

Table S1. Elemental analysis of $AcaCuBr_2$, $AcaCuI_2$, $ImCuBr_2$ and $ImCuI_2$

| | **Cu** | **Br** | **Stoichiometry (Br/Cu)** |
|---|---|---|---|
| $ImCuBr_2$ (point 1) | 33.60 | 66.40 | 1.98 |
| $ImCuBr_2$ (point 2) | 33.48 | 66.52 | 1.99 |
| $ImCuBr_2$ (point 3) | 33.46 | 66.54 | 1.99 |
| **Mean value:** | **33.51±0.08** | **66.49±0.08** | **1.99** |
| $AcaCuBr_2$ (point 1) | 33.55 | 66.45 | 1.98 |
| $AcaCuBr_2$ (point 2) | 33.72 | 66.28 | 1.97 |
| $AcaCuBr_2$ (point 3) | 33.63 | 66.37 | 1.97 |
| **Mean value:** | **33.63±0.09** | **66.37±0.09** | **1.97** |

| | **Cu** | **I** | **Stoichiometry (I/Cu)** |
|---|---|---|---|
| $ImCuI_2$ (point 1) | 40.47 | 59.53 | 1.47 |
| $ImCuI_2$ (point 2) | 40.41 | 59.59 | 1.47 |
| $ImCuI_2$ (point 3) | 41.09 | 58.91 | 1.43 |
| **Mean value:** | **40.66±0.38** | **59.34±0.38** | **1.46** |
| $AcaCuI_2$ (point 1) | 38.26 | 61.74 | 1.61 |
| $AcaCuI_2$ (point 2) | 36.00 | 64.00 | 1.78 |
| $AcaCuI_2$ (point 3) | 35.25 | 64.75 | 1.84 |
| **Mean value:** | **36.50±1.57** | **63.50±1.57** | **1.74** |

| | **Cu** | **I** | **Stoichiometry (I/Cu)** |
|---|---|---|---|
| CuI (point 1) | 55.23 | 44.77 | 0.81 |
| CuI (point 2) | 54.90 | 45.10 | 0.82 |
| CuI (point 3) | 55.15 | 44.85 | 0.81 |
| **Mean value:** | **55.09±0.17** | **44.91±0.17** | **0.81** |

Table S2. Parameters of the crystal structure refinement.

| Phase | $ImCuI_2$ | $ImCuBr_2$ | $AcaCuI_2$ | $AcaCuBr_2$ |
|---|---|---|---|---|
| Empirical formula | $C_9H_{15}I_6Cu_3N_6$ | $C_3H_5Br_2CuN_2$ | $C_2H_7I_2CuN_2$ | $C_2H_7Br_2CuN_2$ |
| $M$, g/mol | 1159.29 | 292.45 | 376.44 | 282.46 |
| Crystal system | Monoclinic | Monoclinic | Orthorhombic | Orthorhombic |
| Space group | $P2_1/m$ | $C2/m$ | $Immm$ | $Immm$ |
| $a$, Å | 8.5159(7) | 15.3264(14) | 6.3429(3) | 6.0639(2) |
| $b$, Å | 14.1096(11) | 8.8529(9) | 8.6068(4) | 8.0448(3) |
| $c$, Å | 10.9304(8) | 11.8454(18) | 14.8678(9) | 14.3987(6) |
| $\alpha$, deg. | 90.000 | 90.000 | 90.000 | 90.000 |
| $\beta$, deg. | 106.810(3) | 118.931(3) | 90.000 | 90.000 |
| $\gamma$, deg. | 90.000 | 90.000 | 90.000 | 90.000 |
| $V$, Å$^3$ | 1257.23(17) | 1406.6(3) | 811.66(7) | 702.41(5) |
| Temperature (K) | 298 | 100.0(2) | 100.0(2) | 100.0(2) |
| $Z$ | 6 | 8 | 4 | 4 |
| $D$ (calc), g/cm$^3$ | 3.062 | 2.762 | 3.081 | 2.671 |
| $\mu$, mm$^{-1}$ | 9.887 | 14.364 | 10.205 | 14.377 |
| $F$(000) | 1032 | 1088 | 672 | 528.0 |
| Crystal size, mm | 0.31×0.26×0.25 | 0.23×0.22×0.18 | 0.21×0.16×0.16 | 0.22×0.19×0.18 |
| $\Theta$ range for data collection, deg. | 1.946 - 30.512 | 2.704 - 30.552 | 2.735 - 30.617 | 5.658 - 54.958 |
| Index ranges | $-12 \le h \le 12$<br>$-20 \le k \le 18$<br>$-15 \le l \le 15$ | $-21 \le h \le 21$<br>$-12 \le k \le 12$<br>$-16 \le l \le 16$ | $-9 \le h \le 9$<br>$-12 \le k \le 12$<br>$-21 \le l \le 21$ | $-7 \le h \le 7$<br>$-10 \le k \le 9$<br>$-18 \le l \le 18$ |
| Reflections collected/independent | 28583 / 3975 | 11940/2261 | 22935/746 | 5025 / 489 |
| $R_{int}$ | 0.0602 | 0.0764 | 0.064 | 0.0471 |
| Reflections with $I>2\sigma(I)$ | 2883 | - | 730 | 489 |
| Goodness-of-fit on $F$ | 1.028 | 1.089 | 1.260 | 1.140 |
| Final $R$ indices [$I>2\sigma(I)$] | $R_1 = 0.0354$<br>w$R_2 = 0.0639$ | $R_1 = 0.0351$<br>w$R_2 = 0.0721$ | $R_1 = 0.0166$<br>w$R_2 = 0.0318$ | $R_1 = 0.0160$<br>$wR_2 = 0.0344$ |
| $R$ indices (all data) | $R_1 = 0.0599$<br>$wR_2 = 0.0721$ | $R_1 = 0.0529$<br>$wR_2 = 0.0797$ | $R_1 = 0.0217$<br>$wR_2 =0.0320$ | $R_1 = 0.0173$<br>$wR_2 =0.0350$ |
| $T_{min}$ / $T_{max}$ | 0.3947 / 0.7461 | 0.472 / 0.746 | 0.589/0.746 | 0.0449/0.0.949 |
| Largest diff. peak/hole, e/Å$^3$ | 1.283 / -0.865 | 1.157/-1.122 | 2.313/-1.961 | 0.42/-0.54 |

Table S3. Optical properties of the studied phases in comparison with other known halocuprates

| Phase | PL maximum, eV | Optical band gap, eV | Stokes Shift, eV | Reference | Measured temperature (PL) |
|---|---|---|---|---|---|
| $AcaCuI_2$ | 2.16 / 2.58 | 2.95 | 1.24* 1.64* | This work | 77 K |
| $AcaCuBr_2$ | 2.67 | 4.03 | 1.65* | This work | 77 K |
| $ImCuI_2$ | 2.30 | 3.45 | 1.64* | This work | 77 K |
| $ImCuI_2$ | 2.24 | 3.45 | 1.51 | This work | 298 K |
| $ImCuBr_2$ | 2.43 | 4.00 | 1.85 | This work | 77 K |
| $PEACuI_2$ | 2.36 | 3.73 | 1.64 | 10.1021/acs.jpcc.1c10402 | 298 K |
| $MBACuBr_2$ | - | 4.10 | - | 10.1002/anie.202115024 | - |
| $PEACuI_2$ | 2.29 | 4.02 | 1.69 | 10.1016/j.mtchem.2023.101408 | 298 K |
| $[(Me)\text{-}Py]CuI_2$ | 2.15 | 2.80 | 1.35 | 10.1039/c9dt01460h | 298 K |
| $MACuBr_2$ | 2.30 | 3.78 | 1.48 | 10.1039/d3dt00687e | 77 K |
| $FACuBr_2$ | 2.53 | 3.88 | 1.35 | 10.1039/d3dt00687e | 77 K |
| MACuIBr | 2.51 | 3.49 | 0.99 | 10.1002/adom.202202952 | 298 K |
| $(Ph_4P)CuCl_2$ | 2.21 | 4.00 | 1.87 | 10.1016/j.jssc.2022.123626 | 298 K |
| $(Ph_4P)CuBr_2$ | 2.36 | 4.00 | 1.86 | 10.1016/j.jssc.2022.123626 | 298 K |

* Stokes shift was calculated as a difference of PL and PLE maxima